Studies in

Applied Electromagnetics and Mechanics

Editors

Volume 14

Previously published in this series:

Vol. 13. In preparation
Vol. 12. T. Takagi, J.R. Bowler and Y. Yoshida (Eds.), Electromagnetic Nondestructive Evaluation
Vol. 11. H. Tsuboi and I. Sebestyen (Eds.), Applied Electromagnetics and Computational Technology
Vol. 10. A.J. Moses and A. Basak (Eds.), Nonlinear Electromagnetic Systems
Vol. 9. T. Honma (Ed.), Advanced Computational Electromagnetics
Vol. 8. R. Collins, W.D. Dover, J.R. Bowler and K. Miya (Eds.), Nondestructive Testing of Materials
Vol. 7. C. Baumgartner, L. Deecke, G. Stroink and S.J. Williamson (Eds.), Biomagnetism: Fundamental Research and Clinical Applications

Volumes 1-6 have been published by Elsevier Science under the series title "Elsevier Studies in Applied Electromagnetics in Materials".

ISSN: 1383-7281

Electromagnetic Nondestructive Evaluation (II)

Edited by

R. Albanese
Università degli Studi di Reggio Calabria, Italy

G. Rubinacci
Università degli Studi di Cassino, Italy

T. Takagi
Tohoku University, Japan

and

S.S. Udpa
Iowa State University, USA

IOS Press
Ohmsha

Amsterdam • Berlin • Oxford • Tokyo • Washington, DC

Electromagnetic Nondestructive Evaluation (II)
R. Albanese et al. (Eds.)
IOS Press, 1998

Evaluation of the Characteristics of a Rotating Eddy-Current Probe for ECT using Edge FEM

Masahiro Hayakawa, Vlatko Čingoski, Kazufumi Kaneda and Hideo Yamashita

Faculty of Engineering, Hiroshima University, 1-4-1 Kagamiyama Higashihiroshima 739, Japan

Abstract. In this paper, the evaluation of the characteristics of a new type rotating eddy-current probe for nondestructive Eddy-Current Testing (ECT) is carried out using 3-D edge-based FEM. The changes of the induced electromotive force are monitored for various inner and outer types of thin cracks inside the metal plate. It was verified that although the intensity of the signal obtained by this new type of probe is smaller than the conventional ones, the shape of the signal and especially its trace could be very useful for detection of the shape, direction and depths of thin cracks and flaws inside thin conducting materials.

1. Introduction

Eddy-Current Testing (ECT) is an efficient nondestructive testing method for detecting surface cracks or flaws in conducting materials. It is very often used for in-service inspection of tubes in steam generators, heat exchangers or condensers for conventional or even more for nuclear power plants or chemical installations, where the security conditions are very taught and must be constantly monitored and strictly satisfied. Due to the fact that in this type of inspection direct contact with test material or any other hazardous elements is completely avoided, ECT could be easily automated. Therefore, for successful ECT different type of sensors such as pan-cake probe, plus-point probe, Cecco-probe, etc., have already been developed with various success [1], [2]. Although the pan-cake probe exhibits the largest ECT signal, the determination of the crack size, its position, depth and width which is also very important is extremely difficult to be achieved using this conventional type of ECT probe due to the fact that the eddy-currents induced by this probe do not easily permeate inside the external conductors.

Recently, a new ECT probe which utilize a rotating eddy-currents was developed for the purpose of carrying out more efficient eddy-current testing [3]. Although physical properties of this type of ECT probe have already been theoretically described [3], evaluation of its properties for detection of thin cracks has not been carried out yet. Therefore, the main purpose of this paper is to evaluate the main characteristics of this new type rotating eddy-current probe by using 3-D numerical analysis and to discuss

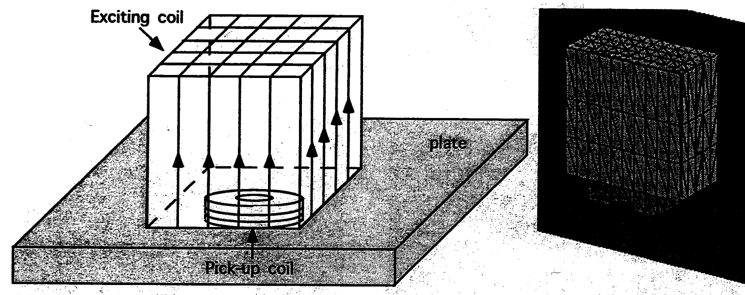

(a) Rotating eddy-current probe. (b) Generated finite element mesh.

Fig. 1: Structure of the rotating eddy-current probe and the finite element mesh.

2. Rotating Eddy-current Probe

The simplified structure of the recently proposed rotating eddy-current probe is shown in Fig. 1a. The probe itself comprises of a small pick-up coil and a pair of exciting coils geometrically rotated for 90° to each other, constructing a cubic shape conductor. Inside each coil the source currents which are electrically 90° off-phase flow inducing uniform rotating eddy-currents inside the conducting plate. The probe has a self-differential feature which eliminates noise effects from variations of electromagnetic characteristics in conducting materials and makes the probe lift-off noise-free. Also, the probe enables detection of almost any type of crack because it directs eddy-currents rotationally in all direction. According to the crack position and its properties, the distribution of eddy-currents and the generated rotated magnetic field changes only locally as shown in Fig. 2. Therefore, the probe detects cracks by measuring electromotive force changes as a result of the local changes in magnetic field and eddy-current distributions around thin cracks.

3. Numerical Analysis Method

Numerical analysis of the characteristics of the probe was carried out in two steps: first step, computation of a 3-D eddy-current distribution inside conducting plate using edge-based FEM, and second step, computation of the changes of the induced electromagnetic force inside the pick-up coil due to the changes of the generated eddy-current distribution around the crack using the Biot-Savart law. First, the entire analysis domain was discretized into mesh of tetrahedral edge finite elements as shown in Fig. 1b, with six degrees of freedom associated with six edges of each finite element and the eddy-current problem was solved according to the following governing equation

$$\nabla \times (\nu \nabla \times \mathbf{A}) = \mathbf{J}_0 - \sigma \frac{\partial \mathbf{A}}{\partial t} \tag{1}$$

where $\mathbf{A}$, $\mathbf{J}_0$, ν, and σ are the magnetic vector potential, the source current density,

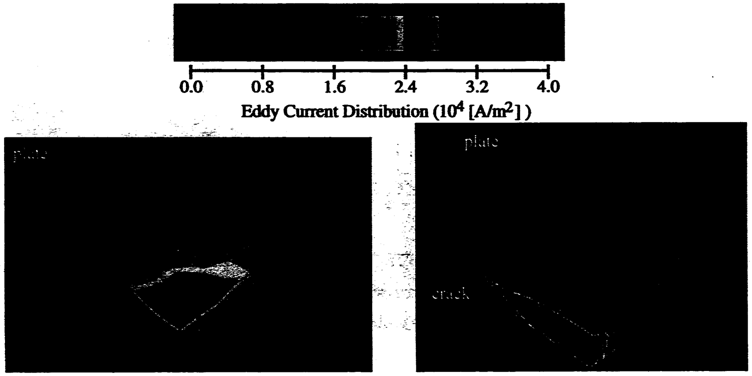

(a) no crack (b) inner crack 60%

Fig. 2: Local eddy-current distribution inside metal plate without and with thin crack.

material, respectively. The eddy current density $\mathbf{J}_{i,e}$ at each integration point i inside each finite element inside the conducting region was calculated as

$$\mathbf{J}_{i,e} = -j\omega\sigma\mathbf{A}_{i,e} \tag{2}$$

In order to detect the existence of a crack inside the conductor, we have to evaluate the signal generated as a result of the changes in the intensity and the phase of the induced electromotive force. Applying the Biot-Savart's law the magnetic vector potential $\mathbf{A}_c$ inside the pick-up coil region can be expressed using the following equation

$$\mathbf{A}_c = \frac{\mu}{4\pi}\sum_{k=1}^{n_e}\sum_{j=1}^{n_i}\frac{w_{j,k}\mathbf{J}_{j,k}V_k}{|\mathbf{r}_{c,j}|} \tag{3}$$

where $w_{j,k}$ is the weight of the j-th integration point of the k-th finite element, V_k is the volume at the k-th element, and $|\mathbf{r}_{c,j}|$ is the distance from the integration point j to the measured point inside the pick-up coil region c. In the above equation n_e, n_i, and μ are the total number of finite elements inside conducting region, the number of integration points per one element, and the permeability coefficient, respectively.

The change of the electromotive force can be computed according to the following equation

$$\mathbf{V} = -j\omega \mathrm{N}_t \int_l \mathbf{A}_c \cdot d\ell \tag{4}$$

where N_t is the total number of turns of the pick-up coil, and l is the contour line of the pick-up coil. In order to optimize the computation time and the accuracy of the results, in our analysis we consider five integration points per each finite element.

4. Simulation Model and Results

For evaluation of the characteristics of a rotated eddy-current probe, we developed a model of square shape metal plate with thin crack along its center. The size of the plate was 40 mm × 40 mm × 1.25 mm with relative permeability and conductivity coefficients equal to 1.0 and 10^6 S/m, respectively. The size of the system of two exciting coils was 5 mm × 5 mm × 5 mm. For modeling of the source current we used eleven current line segments as shown in Fig. 1a with intensity of 1 At, and frequency of 100 kHz. The shape of the pick-up coil was rectangular with inner length of 1.0 mm and the outer length of 3.0 mm, and height of 0.8 mm with total number of turns N_t = 100. The lift-off was 0.5 mm. For simplicity and due to the symmetry of the model, only one half of the analysis model was discretized into finite element mesh and the movement of the ECT probe along the crack direction was enabled.

Four different problems were treated separately in order to verify the output characteristics of the analyzed probe due to the existence of the thin crack:

- *Problem 1* — Signal vs. position of the crack,
- *Problem 2* — Signal vs. depths of the crack,
- *Problem 3* — Signal vs. lengths of the crack, and
- *Problem 4* — Signal vs. shape of the crack.

All four problems were investigated using the obtained signal of the pick-up coil when the probe was moving from the center of the crack towards its end with step of 1 mm along crack direction. In what follows, the results obtained for each problem are presented and discussed separately.

4.1. Problem 1: Signal vs. Position of the crack

Regarding position of the defect (crack) in general two main cases can be considered: inner defect (ID), when the crack and the probe are from the same side of the conducting plate, and outer defect (OD) when the crack and the probe are on the opposite sides. Two models were developed: inner defect model ID60% and outer defect model OD60%. The depth of the crack is usually expressed with percentage of the total thickness of the plate. During simulation, the rotated eddy-current probe was translated along crack direction from the center of the crack towards its end with step of 1 mm. The lengths and widths of the modeled crack was constant and equal to 10 mm and 0.2 mm, respectively. Only half domain was meshed into 35694 tetrahedral elements, and the total number of the nodes and the edges was 6897 and 44385, respectively. The matrix equations were solved by the Incomplete Cholesky Conjugate Gradient (ICCG) Method with convergence criterion of 10^{-5}. The analysis needed about 230 $Mbyte$ of computer memory and about 2400 sec per one measuring point on the SGI Workstation INDIGO-2 IMPACT.

The comparison of the induced electromotive force generated by the probe for inner and outer crack separately is shown in Fig. 3. Figure 3a show the intensity values while Fig. 3b show the trace of the electromotive force. As can be seen from the figures, the shape of the output signal is the same for inner and for outer crack, however its amplitude is almost two times larger for inner crack than for outer crack. This result

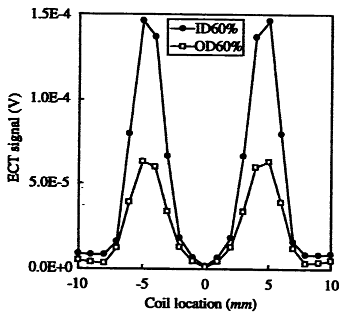

(a) Intensity values of the signal

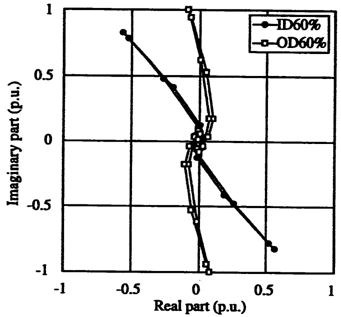

(b) Trace of the signal

Fig. 3: Probe signal vs. position of the crack.

from the same side of the plate. Therefore, local changes of the induced eddy-current distribution around crack area have larger influence over the electromotive force induced inside the probe for inner crack than for outer crack. Second and also very important property of the probe is that as the pick-up coil approaches the edge of the crack, the generated signal becomes larger, while in the center of the crack the signal becomes almost equal to zero due to the symmetrical property of the crack. Therefore, by simple observation of the generated signal and its intensity, one can easily define the position (by the amplitude of the signal), the length (by the distance between both peaks in the signal) and the shape (by the symmetrical shape of the signal) of the crack. The difference between traces of the signal for inner and outer crack as can be seen from Fig. 3b, can be of additional help during evaluation of the crack properties.

4.2. Problem 2: Signal vs. Depths of the crack

As already mentioned in the above paragraph, the electromotive force obtained by the probe enables easy detection of the depths of crack by simple investigation of the signal's amplitude. For example, in Figs. 4 and 5 the obtained signals for inner and outer crack and their traces are given separately for several crack depths: inner cracks $ID60\%$, $ID40\%$ and $ID20\%$, and outer cracks $OD60\%$, $OD40\%$ and $OD20\%$. As can be seen, as the depths of the crack decrease, the amplitude of the signal also decrease, for both inner and outer crack. The amplitude for inner crack is always larger than that of the outer crack for the same crack depths. Finally, from the trace of the signal, one can see that the changes of the trace could be very useful for diagnostic of the crack position and depth as follows: in case of inner crack increment of the crack's depth results in signal which trace rotates in clockwise direction, while in case of outer crack, the trace rotates in anticlockwise direction with increment of the crack depths. Therefore, the depths of the crack can be accurately estimated according to the intensity and trace of the signal.

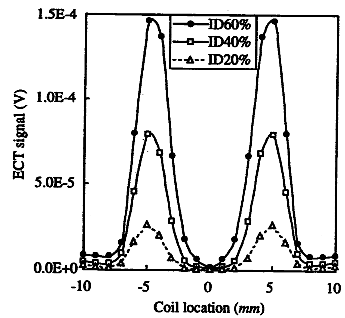

(a) Intensity values of the signal

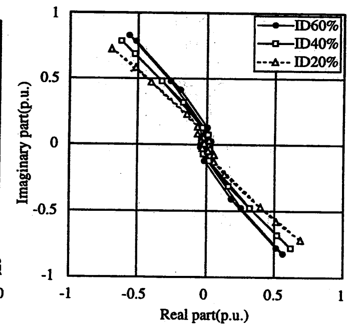

(b) Trace of the signal

Fig. 4: Probe signal vs. depths of the crack: Inner crack (ID).

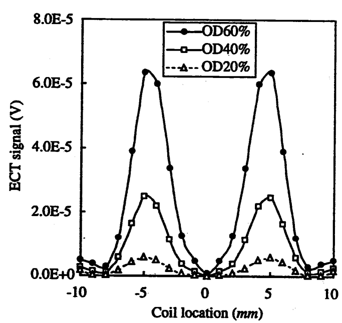

(a) Intensity values of the signal

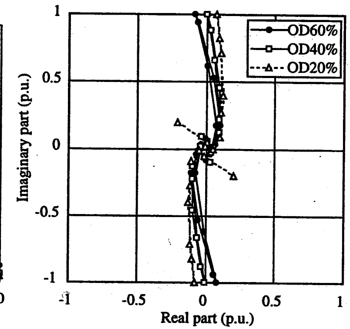

(b) Trace of the signal

Fig. 5: Probe signal vs. depths of the crack: Outer crack (OD).

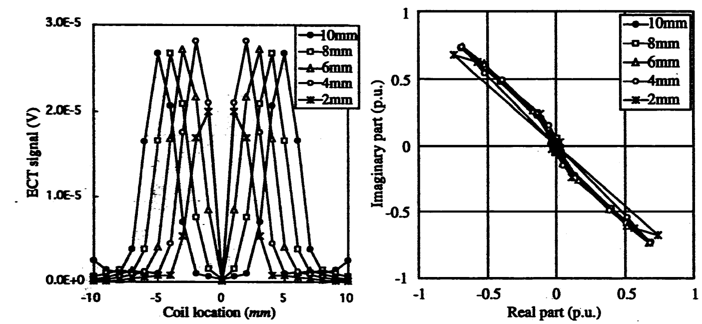

(a) Intensity values of the signal (b) Trace of the signal

Fig. 6: Probe signal vs. lengths of the crack for $ID20\%$.

4.3. Problem 3: Signal vs. Lengths of the crack

Modeling of several cracks with different length was used in order to investigate the sensitivity of the probe due to the existence of cracks with various lengths. The probe movement was again simulated along the crack direction with step of 1 *mm* using the same finite element mesh utilized in previous problems. Five different models were developed, for both inner $ID20\%$ and outer $OD20\%$ cracks with the following lengths: 10, 8, 6, 4, and 2 *mm* and width of only 0.2 *mm*.

The obtained results for the electromotive force changes are shown in Figs. 6 and 7, for inner and outer crack, respectively. Figures 6a and 7a show the changes in the intensity values of the induced electromotive force, while Figs. 6b, and 7b show the changes in the trace of the electromotive force. As can be seen, the distance between peaks of the signal give the exact information for the length of the crack. However, small difference in the signal obtained for the inner and outer cracks with lengths of 2 *mm* can be observe in comparison with other signals. This result can be attributed to the size of the pick-up coil, and we may conclude that when the lengths of the crack is shorter or its lengths is of the same order with the size of the pick-up coil, the detection of the crack could be more difficult and less accurate results could be expected.

4.4. Problem 4: Signal vs. Shape of the crack

Probably the most difficult problem of all is to define accurately the shape of the crack according to the obtained signal for induced electromotive force. In order to investigate the possibilities of shape detection, two simple models with stepwise crack shape were developed as shown in Fig. 8. The first model crack had symmetrical stepwise shape with only two different depths, $ID40\%$ at center of the crack with length of 4 *mm*, and two $ID20\%$ areas placed on both sides of the central crack with lengths of 3 *mm* each as shown in Fig. 8a. The second model crack also shown in Fig. 8b, had asymmetrical stepwise shape with three different depths, $ID60\%$, $ID40\%$, and $ID20\%$, with first and

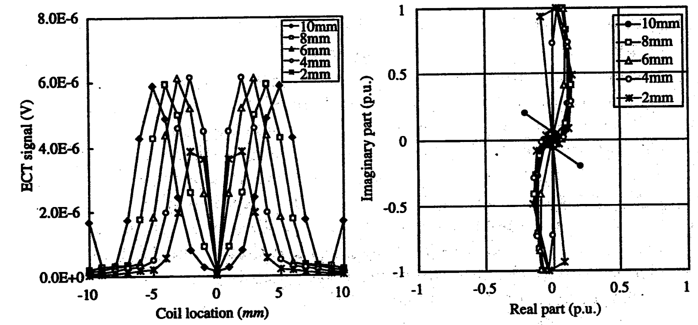

(a) Intensity values of the signal (b) Trace of the signal

Fig. 7: Probe signal vs. lengths of the crack for $OD20\%$.

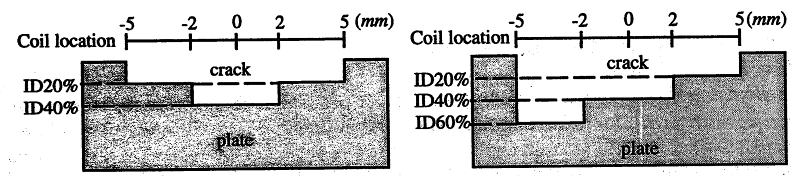

(a) Symmetrical stepwise crack (b) Asymmetrical stepwise crack

Fig. 8: Structure of the model cracks.

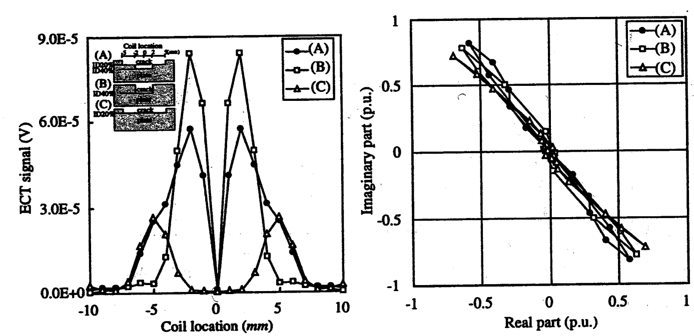

(a) Intensity values of the signal (b) Trace of the signal last being 3 *mm* long and the second one being 4 *mm* long. Again, we simulated the signal of the probe obtained due to the uniform translation of the probe along cracks direction with step of 1 *mm* using the same finite element mesh as above.

The obtained signals for the electromotive changes are shown in Figs. 9 and Figs. 10, respectively. Figure 9 shows a comparison between the obtained signal for symmetrical stewise crack and previously obtained signals for cracks with constant depths $ID20\%$ and $ID40\%$. As can be seen the signal for stepwise crack is positioned between signals for cracks with constant depths $ID40\%$ and $ID20\%$. Additionally, in the central area the signal have the same shape as constant crack $ID40\%$ only with smaller amplitude, while at its ends the shape of the signal becomes like that of the $ID20\%$ crack. Therefore, user with some experience could easily distinguish between constant and stepwise crack by the shape, position and intensity of signal's amplitude.

On the other side, detection of an asymmetrical stepwise crack as can be seen from Fig. 10 is very difficult using this type of probe. First of all, as a result of the crack's asymmetrical shape the intensity of the signal at the center does not become zero. The shape of the signal is asymmetrical with several peaks and drops making extremely difficult to estimate the lengths and depths of the crack. However, using predefined table of generated signals for various type of possible defects, it is possible to determine to some extend the shape, depths and lengths of this type of crack by comparison with more simple crack types.

5. Discussions and Concluding Remarks

We made an effort to numerically evaluate the properties of a new type of rotating eddy-current probe for ECT and detection of thin cracks or flaws inside metal plates. Using 3-D edge-based finite element method the evaluation of eddy-current distribution inside the metal plate was initially carried out, followed by the computation of induced electromotive force inside the pick-up coil by means of Biot-Savart law. The obtained signals were investigated and classified due to the different properties of the analyzed cracks.

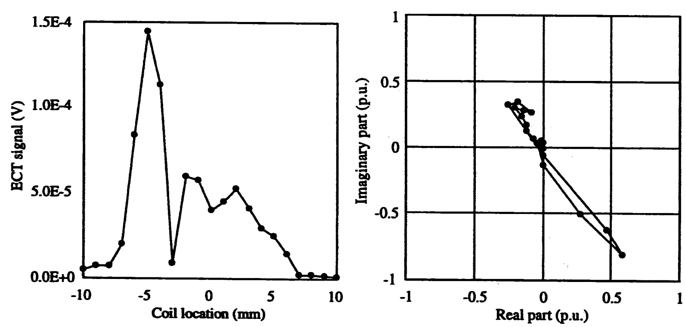

(a) Intensity values of the signal (b) Trace of the signal

Fig. 10: Probe signal vs. shape of the crack: asymmetrical stepwise crack

It was shown that the general properties of this new probe are very promising and advantageous compared with traditional ECT probes. Although the intensity of the output signal is smaller than some other conventional probes, the shape of the signal and its trace could be very useful for detection of the crack existence and crack parameters. It was shown that according to the signal's amplitude, position of the peaks in the signal, its symmetrical shape and trace, one can easily determinate not only the existence of the crack inside the conductor, but also the position, length, depth and even the shape of the crack. The probe reaches its detection limits according to the size of its pick-up coil. The accuracy of the results decreases if the length of the crack is of the same or even smaller order than the actual size of the pick-up coil. The probe also shows some limitation for detection of cracks with asymmetrical and complex geometrical shape. For this type of problems further investigation of the probe and its characteristics is necessary.

References

[1] T. Takagi et al: "Benchmark Models of Eddy Current Testing for Steam Generator Tube: Experiment and Numerical Analysis," *Int. J. of Applied Electromagnetics in Materials*, 5, 1994, pp.149-162.

[2] T. Takagi: "Electromagnetic NDE Research Activities in JSAEM," *Electromagnetic Nondestructive Evaluation, Studies in Applied Electromagnetics and Mechanics, Proceedings of E'NDE*, Tokyo, 1996.

[3] H. Hoshikawa and K. Koyama: "Basic Study of a New ECT Using Uniform Rotating Direction Eddy Current," *Review of Progress in Quantitative Nondestructive Evaluation*, Vol.16, 1997, pp.1067-1074 .